PCCP



PAPER View Article Online View Journal | View Issue



Cite this: Phys. Chem. Chem. Phys., 2021. 23, 17663

Influence of the terminal group on the thermal decomposition reactions of carboxylic acids on copper: nature of the carbonaceous film

Robert Bavisotto, Resham Rana, Nicholas Hopper, Kaiming Hou and Wilfred T. Tysoe **

The effect of the terminal groups on the nature of the films formed by the thermal decomposition of carboxylic acids on copper is studied in ultrahigh vacuum using temperature-programmed desorption (TPD), scanning tunneling microscopy (STM) and Auger electron spectroscopy (AES). The influence of the presence of vinyl or alkynyl terminal groups and chain length is studied using heptanoic, octanoic, 6-heptenoic, 7-octenoic, 6-heptynoic and 7-octynoic acids. The carboxylic acids form strongly bound carboxylates following adsorption on copper at room temperature, and thermally decompose between ~500 and 650 K. Previous work has shown that this occurs by the carboxylate plane tilting towards the surface to eliminate carbon dioxide and deposit a hydrocarbon fragment. The fragment can react to evolve hydrogen or form oligomeric species on the surface, where the amount of carbon increases for carboxylic acids that contain terminal functional groups that can anchor to the surface. These results will be used to compare with the carbonaceous films formed by the mechanochemical decomposition of carboxylic acids on copper, which occurs at room temperature. This is expected to lead to less carbon being deposited on the surface than during thermal decomposition.

Received 11th May 2021, Accepted 1st August 2021

DOI: 10.1039/d1cp02078a

rsc.li/pccp

1. Introduction

Molecules that can form self-assembled monolayers (SAMs) combine a surface anchoring group, often a thiol, ¹⁻⁷ that adsorbs strongly to the substrate, with a long-chain hydrocarbon for which the intermolecular van der Waals' interactions impart stability to the film. Their unique properties have been exploited for many applications ^{1,5,8-10} from chemical anchors on nanoparticles for drug delivery, ¹¹ as sensors, ^{12,13} for molecular electronics, ¹⁴⁻¹⁷ or for preventing adhesion in microelectromechanical system (MEMS). ^{18,19} SAMs formed from carboxylic, or fatty acids have been used as so-called boundary lubricants ²⁰⁻²⁴ by adsorbing strongly to the surface to prevent adhesion between the contacting surfaces. ²⁵ However, the carboxylic SAMs can also decompose under the influence of sliding shear to form low-friction carbonaceous layers. ²⁶⁻³⁰

It has been shown previously that C_7 and C_8 carboxylic acids adsorb onto a copper surface at room temperature by deprotonating to form a carboxylate that binds to the surface through both oxygens in a bidentate structure. At lower coverages, the hydrocarbon group can interact with the copper substrate to lay flat on the surface. At higher coverages, the intermolecular van

der Waals' induce an upright geometry with the chain terminus remote from the surface. Finally, the adsorbed carboxylates thermally decompose to evolve carbon dioxide on heating to above ~ 600 K. $^{31-38}$ In contrast, acetate species on copper mechanically decompose during rubbing at room temperature 39 to either evolve carbon dioxide as in the thermal reaction, or to desorb carbon monoxide and deposit oxygen on the surface in a shear-induced reaction pathway.

Since mechanochemical reactions are induced at lower temperatures by sliding than the thermal reaction, it might be expected that the interaction of the terminus of the hydrocarbon chain with both the substrate as well as the nature of the sliding counterface might influence the reactivity. 40 As a basis for ultimately exploring these effects, the goal of this work is to study the thermal reaction pathways of a number of carboxylic acids adsorbed on copper with different alkyl, vinyl, or alkynyl terminal groups with a particular focus on the influence of the terminal groups on the nature of the carbonaceous overlayer. These results will enable the chemistry of the thermally and mechanically formed films to be compared. Presented here are experiments carried out using heptanoic and octanoic acids as example of alkyl-terminated SAMs, 6-heptenoic and 7-octenoic acids for vinyl-terminated SAMs, and 6-heptynoic and 7-octynoic acids as acetylide-terminated molecules.

Department of Chemistry, University of Wisconsin-Milwaukee, Milwaukee, WI 53211. USA. E-mail: wtt@uwm.edu

Paper

The surface chemical reactions are investigated using temperature-programmed desorption (TPD), scanning tunneling microscopy (STM) and Auger electron spectroscopy (AES). A clean copper foil was used for the TPD and AES experiments to more closely compare to subsequent tribological studies, where use of single crystals would be prohibitively expensive. STM experiments were carried using a Cu(100) single crystal.

2. Experimental

Experiments were carried out in UHV chambers operating at base pressures of $\sim 2.0 \times 10^{-10}$ Torr after bakeout. TPD experiments were carried out using a Dycor M200M quadrupole mass spectrometer, which was enclosed in a metal shield to prevent signals from the sample supports from reaching the mass spectrometer. The C₇ and C₈ carboxylic acids, which have relatively low vapor pressures, were dosed from a Knudsen source. The exposure duration was varied for each acid, allowing different surface coverages to be obtained. The coverage of each carboxylic acid was measured from carbon/copper peak-to-peak ratios in the Auger spectra and subsequently compared with the carbon/copper peak-to-peak ratio of the carbon-covered surface produced after the TPD experiments. The temperature was ramped at a rate of 5 K s⁻¹ for each experiment and AES spectra were taken immediately after heating. The sequential TPD and AES experiments were performed in the same manner, but the sample was allowed to cool to room temperature before exposure to the carboxylic acid. It is important to note that each of these experiments was performed without cleaning the sample between experiment. STM experiments were carried out using an RHK UHV 350 dual AFM/STM using a sharp tungsten tip. The surface was exposed to the corresponding carboxylic acid at 300 K to obtain a saturated overlayer and annealed to 850 K in UHV. The samples were allowed to cool to room temperature and then moved onto the scanning stage for STM measurements.

The copper foil sample used for the TPD and AES experiments was prepared by mechanically polishing using sandpapers of increasingly fine grit. This was followed by polishing using polycrystalline diamond paste in descending size until 1 μm. This resulted in a visibly smooth surface under a microscope. The sample was mounted in UHV to a precision x, y, z, φ manipulator and cleaned using a standard procedure that consisted of Ar⁺ bombardment with subsequent annealing to 850 K for 10 minutes. Ion bombardment was performed at a background gas pressure of $\sim 3.0 \times 10^{-5}$ Torr of argon at a 2 kV potential while maintaining a \sim 2 μ A sample current. This process was repeated until the sample was determined to be sufficiently clean by AES where, in particular, no carbon and oxygen were detected on the surface. The Cu(100) single crystal used in the STM experiments was cleaned by Ar⁺ bombardment for 30 minutes. This was followed by annealing at 875 K for 30 minutes. This cleaning procedure was repeated until the sample was found to be clean by AES.

Each carboxylic acid (Sigma Aldrich, >95% purity) was purified using several freeze-pump-thaw cycles and their purities were judged by mass spectrometry and were dosed onto the

surface using a Knudsen source with an attached tube of 3.2 mm internal diameter placed in close proximity to the front of the sample. This arrangement limits the contamination of other parts of the UHV chamber and enhances the local pressure close to the sample.

3. Results

The temperature-programmed desorption experiments were performed for heptanoic, 6-heptenoic, 6-heptynoic, octanoic, 7-octenoic and 7-octynoic acids adsorbed on clean copper foils at 300 K and the results are displayed in Fig. 1 for the 44 amu (CO₂) signal and in Fig. 2 for the 2 amu (H₂) profiles for each acid as a function of relative coverage of the corresponding carboxylate. Other masses, such as the 28 amu (CO) fragment, were also monitored. The 28 amu signal coincided with the 44 amu peak and was assigned to a carbon dioxide fragment. Larger mass fragments corresponding to hydrocarbon products were monitored, but their signals were weak due to the decreased mass spectrometer sensitivity at higher masses.

All carboxylic acids undergo decarboxylation between ~ 500 and 700 K as evidenced by the CO2 formation (Fig. 1), where previous work has indicated that the reaction occurs by the plane of the carboxylate tilting towards the surface to weaken the C-COO bond to eject carbon dioxide.³⁹ The desorption profile consists of two features. A low-temperature state appears between ~500 and 550 K at low coverages for each carboxylic acid, which is attributed to the decomposition of a carboxylate species that has been identified previously at low coverages for which the carbon chain terminus can interact with the copper surface to cause the carboxylate group to tilt such that it moves towards the transition-state structure, thereby lowering the reaction activation barrier. 38,41 As the surface becomes more crowded, this induces the formation of a self-assembled monolayer that causes the carboxylic acid to be more vertical to increase the reaction activation energy thereby causing the carbon dioxide desorption temperature to increase.

A significant amount of hydrogen is also evolved during TPD (Fig. 2), which can be categorized depending on whether the hydrogen desorption temperature is below, at the same temperature as, or at a higher temperature than carbon dioxide desorption. For comparison, the locations of the peaks of the most intense 44 amu desorption profiles are indicated by vertical lines in Fig. 2. In particular, the acetylide-terminated carboxylates, 6-heptynoic acid (Fig. 2E) and 7-octynoic acid (Fig. 2F) show no hydrogen evolution prior to the production of CO2. In the case of the alkyl-terminated carboxylates, heptanoic acid (Fig. 2A) and octanoic acid (Fig. 2B), hydrogen evolves prior to the most intense hydrogen desorption feature that occurs simultaneously with CO2 production, and a small amount of hydrogen is evolved at higher temperatures. In the case of vinylterminated carboxylates, 6-heptenoic acid (Fig. 2C) and 7-octenoic acid (Fig. 2D), there is no distinct hydrogen desorption peak directly associated with the formation of CO2, but large hydrogen

PCCP

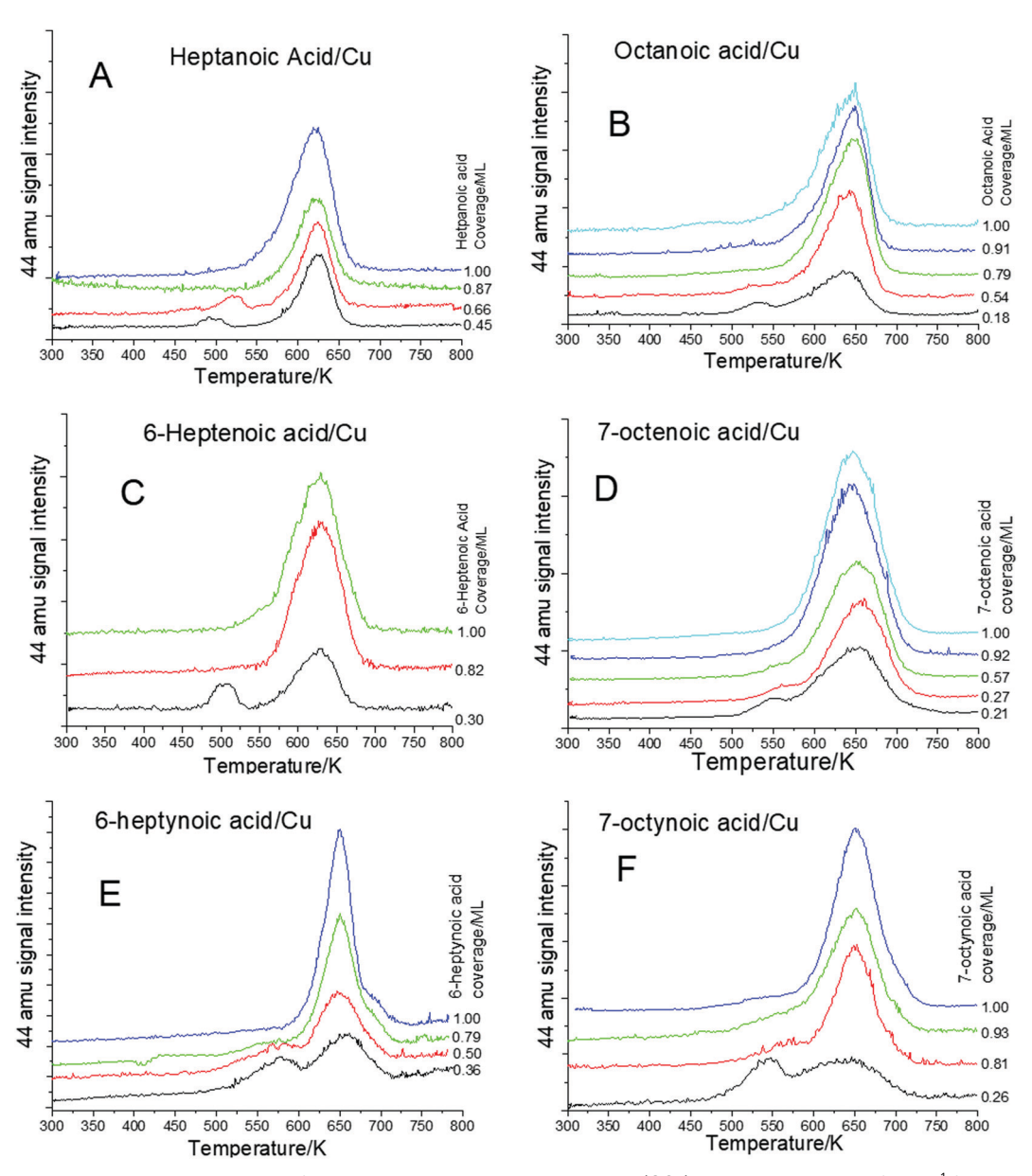


Fig. 1 Temperature-programmed desorption profiles collected while monitoring 44 amu (CO_2) using a heating rate of 5 K s⁻¹ following the adsorption of (A) heptanoic acid, (B) 6-heptanoic acid, (C) 6-heptanoic acid, (D) octanoic acid, (E) 7-octanoic acid, (F) 7-octanoic acid, on a copper foil at 300 K as a function of relative coverage, where the coverages are displayed adjacent to the corresponding spectrum.

peaks appear centered at ~ 600 K, followed by a broad feature extending from \sim 650 to 770 K.

The amount of carbon deposited on the surface was measured using Auger spectroscopy from the C/Cu Auger peak ratio after heating a saturated overlayer to ~ 850 K and compared to the Auger signal following adsorption at 300 K. The results are displayed in Fig. 3A, which show that the amount of carbon deposited on the surface from for C₇ and C₈ carboxylates increases with an increase in unsaturation of the terminal group. No oxygen was found on the surface.

It has been shown previously that ethylene adsorbs in a π -bonded structure on copper with a binding energy of $\sim 36 \text{ kJ mol}^{-1}$ and in a di- σ geometry with an energy of \sim 59 kJ mol⁻¹, ⁴² while acetylene desorbs with an activation energy of $\sim 70 \text{ kJ mol}^{-1.43}$

These differences in C=C and C≡C surface binding are in accord with the trend in carbon coverage shown in Fig. 3A, which is influenced by the nature of the terminal group. This idea is confirmed by the data shown in Fig. 3B, which plots the percentage of carbon deposited on the surface for the reaction of an adsorbed heptanoate overlayer as a function of initial coverage. Here, the proportion that decomposes is larger at low coverages, where the terminal group can more easily access the surface.

In order to investigate the nature of the resulting carbonaceous species, STM images were collected for copper surfaces saturated with octanoic acid, 7-octenoic acid and 7-octynoic acid after heating the carboxylate overlayer to 850 K, and cooling to room temperature, after which STM images were collected as shown in

PCCP Paper

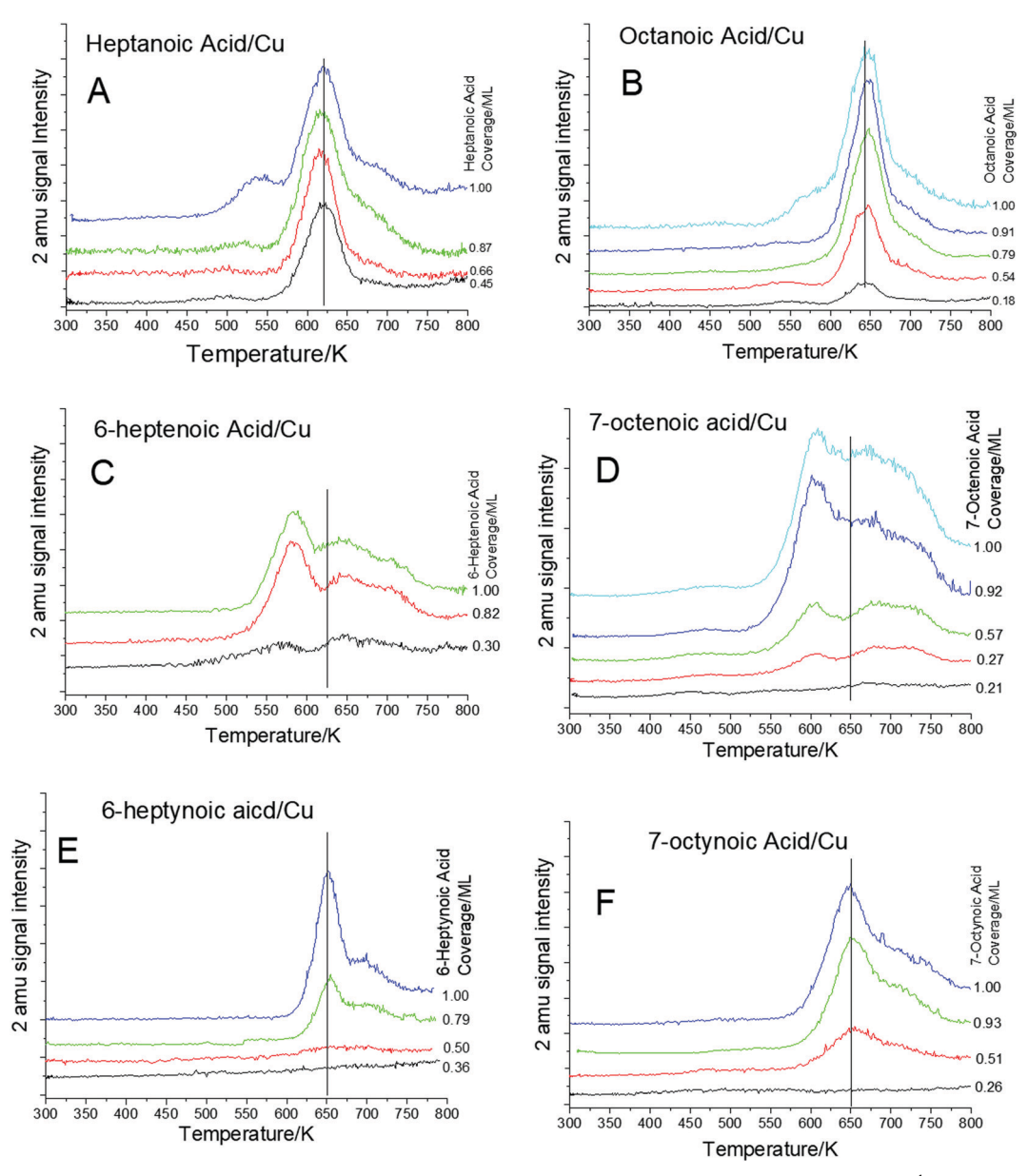


Fig. 2 Temperature-programmed desorption profiles collected while monitoring 2 amu (H₂) using a heating rate of 5 K s⁻¹ following the adsorption of (A) heptanoic acid, (B) 6-heptanoic acid, (C) 6-heptynoic acid, (D) octanoic acid, (E) 7-octenoic acid, (F) 7-octynoic acids on a copper foil at 300 K as a function of relative coverage, where the coverages are displayed adjacent to the corresponding spectrum.

Fig. 4A-C for octanoic acid, Fig. 4D-F for 7-octenoic acid and G and H for 7-octynoic acid on Cu(100). The STM images of octanoic acid (Fig. 4A-C) show some polymeric structures located at terraces, while the majority of the polymer structures are sufficiently mobile at this temperature to be able to diffuse to step edges and agglomerate there. The STM images of a saturated monolayer of 7-octenoic acid after heating to 850 K (Fig. 4D-F) has slightly more polymer visible on the surface than that derived from octanoic acid, in agreement with the AES C/Cu ratios shown in Fig. 3A. The remaining polymeric features occur on both step sites and terraces, being more abundant on terrace sites than the polymers formed from octanoic acid. This is in accord with the idea that the presence of a terminal carbon-carbon double bond enables the hydrocarbon to anchor to the surface resulting in somewhat lower mobility.

The STM images obtained by heating and 7-octynoate overlayer to ~850 K (Fig. 4G and H) exhibit much more polymer on the surface than the film formed by octanoic or 7-octenoic acids, also in agreement with measurements of the amount of carbon on the surface from the Auger data shown in Fig. 3A. The majority of the carbonaceous species are visible on the terraces with only a relatively small proportion agglomerating on step sites.

Since mechanochemical reactions occur in the presence of the reactant, the evolution of the surface with repeated dosing and heating when covered by octanoic, 7-octenoic and 7-octynoic acid was investigated. Here, sequential TPD profiles were collected for surfaces saturated at room temperate with each carboxylic acid without intervening cleaning between experiments for seven

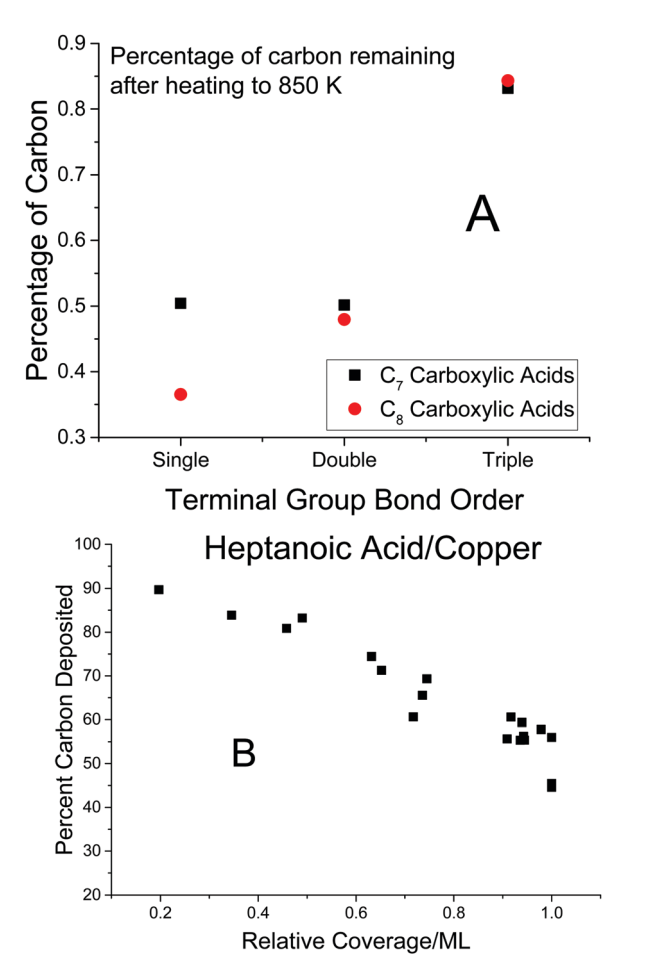


Fig. 3 (A) The variation in the proportion of carbon remaining on the surface after heating a saturated overlayer to 850 K, measured from the C/Cu peal-to-peak Auger ratio, as a function on the nature of the terminal group of the hydrocarbon chain for a series of C_7 and C_8 hydrocarbons. (B) The proportion of carbon remaining on the surface after heating a saturated overlayer of heptanoic acid on copper to 850 K as a function of the initial heptanoic acid coverage.

cycles. The results are displayed in Fig. 5 where the numbers adjacent to each profile indicate the cycle number where Cycle 1 represents adsorption on the initially clean surface. Fig. 5A, C and E show the hydrogen (2 amu) desorption profiles and Fig. 5B, D and F display the profiles for carbon dioxide formation. It is observed that each adsorption-heating cycle yields less hydrogen and carbon dioxide, so that after seven cycles the copper surface is almost completely passivated. The 2 amu (hydrogen) peak shifts to higher temperatures with each iteration showing that the dehydrogenation reactions become more difficult on the carbon-covered surface. In contrast, the $\rm CO_2$ (44 amu) desorption peak temperature shifts only very slightly for octanoic and 7-octynoic acid adsorption, but slightly more for the reaction of 7-octenoic acid on copper.

The results of the corresponding Auger analyses are shown in Fig. 6, which plots the peak-to-peak C/Cu Auger ratio for each experimental cycle and show that a significant amount of carbon adsorbs on the copper surface even after the first carboxylic acid dose. The amount of additional carbon, and

the hydrogen and carbon dioxide yields (Fig. 5) decrease after the first cycles and the total carbon coverage saturates after four cycles of octanoic acid dosing and heating, five cycles with 7-octenoic acid, and six cycles with 7-octynoic acid. The total amount of carbon that can be accommodated on the surface increases with the presence of unsaturation at the terminus of the hydrocarbon moiety and saturates at a C/Cu Auger ratio of ~ 1 for octanoic acid (Fig. 6A), and increases to ~ 1.5 for 7-octenoic and 7-octynoic acid (Fig. 6B and C). The carbon depth profile was estimated from ion-bombarded samples as a function of sputter time using Auger spectroscopy (Fig. 6D-F), which suggests that some carbon has thermally diffused into the substrate, where the sputter times (630 \pm 70 s) required to remove all carbon were identical for all carboxylic acids at. The penetration depth was estimated by saturating the surface with octanoic acid overlayer and by measuring the variation in Auger signal as a function of ion bombardment time under the same condition as used for the experiments in Fig. 6D-F. This approach implicitly assumes that all forms of carbon are removed equally by ion bombardment, and yields a time to remove the C_8 layer of 264 \pm 30 seconds to produce an estimate for the time to remove a monolayer of carbon of 33 \pm 4 seconds, indicating that the data in Fig. 6 corresponds to a carbon depth equivalent to \sim 19 \pm 3 monolayers.

4. Discussion

It has been found previously that carboxylic acids adsorb on copper at room temperature by deprotonating to form η^2 carboxylates with the carboxylate oxygen atoms both binding equivalently to the surface. At lowest coverages, the chain of the C_8 carboxylic acid can tilt towards and interact with the surface. At higher coverages, the carboxylic acid chain stands vertical from the surface with the terminus remote, likely due to van der Waals interactions with its molecular neighbors. 31,33-35,38,41 They thermally decompose by the carboxylate group titling towards the surface until the C-COO- bond weakens sufficiently to eliminate gas-phase carbon dioxide at \sim 650 K, ^{38,41} as illustrated in Fig. 1, to deposit the resulting alkyl species on the surface. This process occurs with an activation energy of \sim 180 kJ mol⁻¹. As the carboxylate group tilts to induce decomposition, this can allow the terminus of the hydrocarbon chain to interact with the surface and thus influence the reactivity of the adsorbed carboxylate. In particular, it can initiate decarbonylation reactions at lower temperatures when the carboxylate coverages are low when the hydrocarbon chain can more easily access the surface. 38,41 This manifests itself as carbon dioxide forming with a lower activation barrier, resulting in carbon dioxide desorption at lower temperatures. This effect is evident in Fig. 1, where small CO2 peaks are detected at \sim 525 K for alkyl-terminated carboxylate (Fig. 1A and B), between 500 and 550 K for vinyl-terminated chains (Fig. 1C and D), and quite large peaks at ~ 525 to 550 K for chains with triple bonds (Fig. 1E and F). There may also be some chain-length effects due to differences in the terminal stereochemistry. At higher

Paper

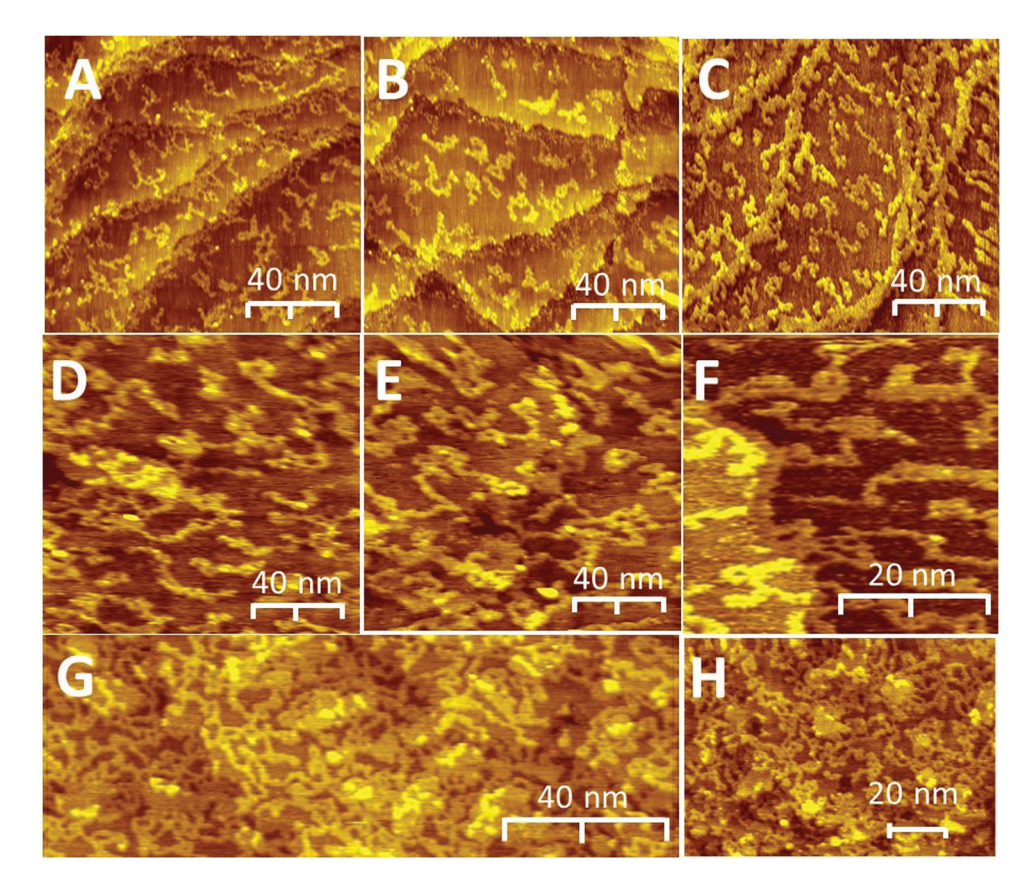


Fig. 4 Scanning tunneling microscope (STM) images of a saturated overlayer of various carboxylic acid adsorbed at 300 K on Cu(100) and heating to 850 K. (A–C) 140 nm \times 140 nm image of octanoic acid ($V_b = -0.75 \text{ V}$, $I_t = 0.100 \text{ nA}$), (D–F) 140 nm \times 140 nm image of 7-octenoic acid ($V_b = -0.75 \text{ V}$, $I_t = 0.100 \text{ nA}$), (D–F) 140 nm \times 140 nm image of 7-octenoic acid ($V_b = -0.75 \text{ V}$, $I_t = 0.100 \text{ nA}$), (D–F) 140 nm \times 140 nm image of 7-octenoic acid ($V_b = -0.75 \text{ V}$, $I_t = 0.100 \text{ nA}$), (D–F) 140 nm \times 140 nm image of 7-octenoic acid ($V_b = -0.75 \text{ V}$, $I_t = 0.100 \text{ nA}$), (D–F) 140 nm \times 140 nm image of 7-octenoic acid ($V_b = -0.75 \text{ V}$, $V_t = 0.100 \text{ nA}$), (D–F) 140 nm \times 140 nm image of 7-octenoic acid ($V_b = -0.75 \text{ V}$, $V_t = 0.100 \text{ nA}$), (D–F) 140 nm \times 140 nm image of 7-octenoic acid ($V_b = -0.75 \text{ V}$, $V_t = 0.100 \text{ nA}$), (D–F) 140 nm \times 140 nm image of 7-octenoic acid ($V_b = -0.75 \text{ V}$), ($V_b = -0.75 \text{$ I_t = 0.094 nA), (G) 55 nm \times 160 nm image of 7-octynoic acid (V_b = -0.76 V, I_t = 0.099 nA), and (H) 110 nm \times 80 nm image of 7-octynoic acid (V_b = -0.76 V, I_t = 0.094 nA), and (H) 110 nm \times 80 nm image of 7-octynoic acid (V_b = -0.76 V, I_t = 0.099 nA), and (H) 110 nm \times 80 nm image of 7-octynoic acid (V_b = -0.76 V, I_t = 0.099 nA), and (H) 110 nm \times 80 nm image of 7-octynoic acid (V_b = -0.76 V, I_t = 0.099 nA), and (H) 110 nm \times 80 nm image of 7-octynoic acid (V_b = -0.76 V, I_t = 0.099 nA), and (H) 110 nm \times 80 nm image of 7-octynoic acid (V_b = -0.76 V, I_t = 0.099 nA), and (H) 110 nm \times 80 nm image of 7-octynoic acid (V_b = -0.76 V, I_t = 0.099 nA), and (H) 110 nm \times 80 nm image of 7-octynoic acid (V_b = -0.76 V, I_t = 0.099 nA), and (H) 110 nm \times 80 nm image of 7-octynoic acid (V_b = -0.76 V, I_t = 0.099 nA), and (H) 110 nm \times 80 nm image of 7-octynoic acid (V_b = -0.76 V, I_t = 0.099 nA), and (H) 110 nm \times 80 nm image of 7-octynoic acid (V_b = -0.76 V, I_t = 0.099 nA), and (H) 110 nm \times 80 nm image of 7-octynoic acid (V_b = -0.76 V, I_t = 0.099 nA), and (H) 110 nm \times 80 nm image of 7-octynoic acid (V_b = -0.76 V, I_t = 0.099 nA), and (H) 110 nm \times 80 nm image of 7-octynoic acid (V_b = -0.76 V, I_t = 0.099 nA), and (I_t = -0.76 V, I_t = -0.76 V, I_t = 0.099 nA), and (I_t = -0.76 V, I_t = -0.76 V, I_t = 0.099 nA), and (I_t = -0.76 V, I_t = -0.76 $I_{\rm t} = 0.097 \, \rm nA)$

coverages, up to saturation, decarbonylation occurs at temperatures of \sim 650 K. In this case, there is not a strong dependence of the CO₂ formation temperature on the nature of the terminal group, but there is some effect on the chain length, where the longer-chain C₈ carboxylates decompose at slightly higher temperatures than the C7 ones due to the larger interchain van der Waals' interactions of ~ 4 kJ mol⁻¹ per methylene group.44,45

The fact that the hydrocarbon fragment is reactively formed at \sim 650 K can influence the subsequent reactivity. The surface chemistry of alkyl species has been studied on transition-metal surfaces,46 and specifically on copper, by forming them at low temperatures by reaction with iodine-containing precursors.47,48 Here, the weak C-I bonds cleave at low temperatures to form an intact alkyl species, in contrast to the carboxylates where the alkyl species are formed at temperature above which they would normally decompose. These experiments reveal that the most facile reaction for alkyl decomposition is via β-hydride elimination to form an alkene at \sim 200 to 250 K in TPD, and is many orders of magnitude faster than α-hydride elimination processes. Coupling reactions between alkyl chains can also occur at ~430 K to form longer-chain hydrocarbons, which, in the case of the C8 and C7 carboxylates studied here produce carbonaceous oligomers on the surface, which are \sim 2 nm long. Note that relative reaction rates increase more rapidly for high-activation-energy process with temperature than for low-activation-energy ones. This means that more carbonaceous oligomers are expected on the surface when the alkyl species are formed at higher temperatures, such as by carboxylate decomposition, than when they are formed at lower temperatures such as by decomposition of a reactive precursor, such as an alkyl iodide, or mechanically, where the reaction can occur at room temperature.39

The fate of the carbonaceous species formed by carboxylate decomposition is also likely to be influenced by the nature of the terminal group. For example, β-hydride elimination from an adsorbed alkyl species will yield a corresponding alkene and remove carbon from the surface. In contrast, the presence of a terminal anchoring group would sterically inhibit the desorption of the resulting alkene and allow it to undergo additional reactions to form surface carbonaceous species. These effects are illustrated in Fig. 3, where Fig. 3A shows that the amount of carbon deposited on the surface increases with the presence of unsaturation of the terminal carbons, with an acetylide group being more reactive than a vinyl group. The effect of the ability of the terminal group to access the surface is shown in Fig. 3B, which illustrates that the proportion of the carbon remaining on the surface depends

PCCP

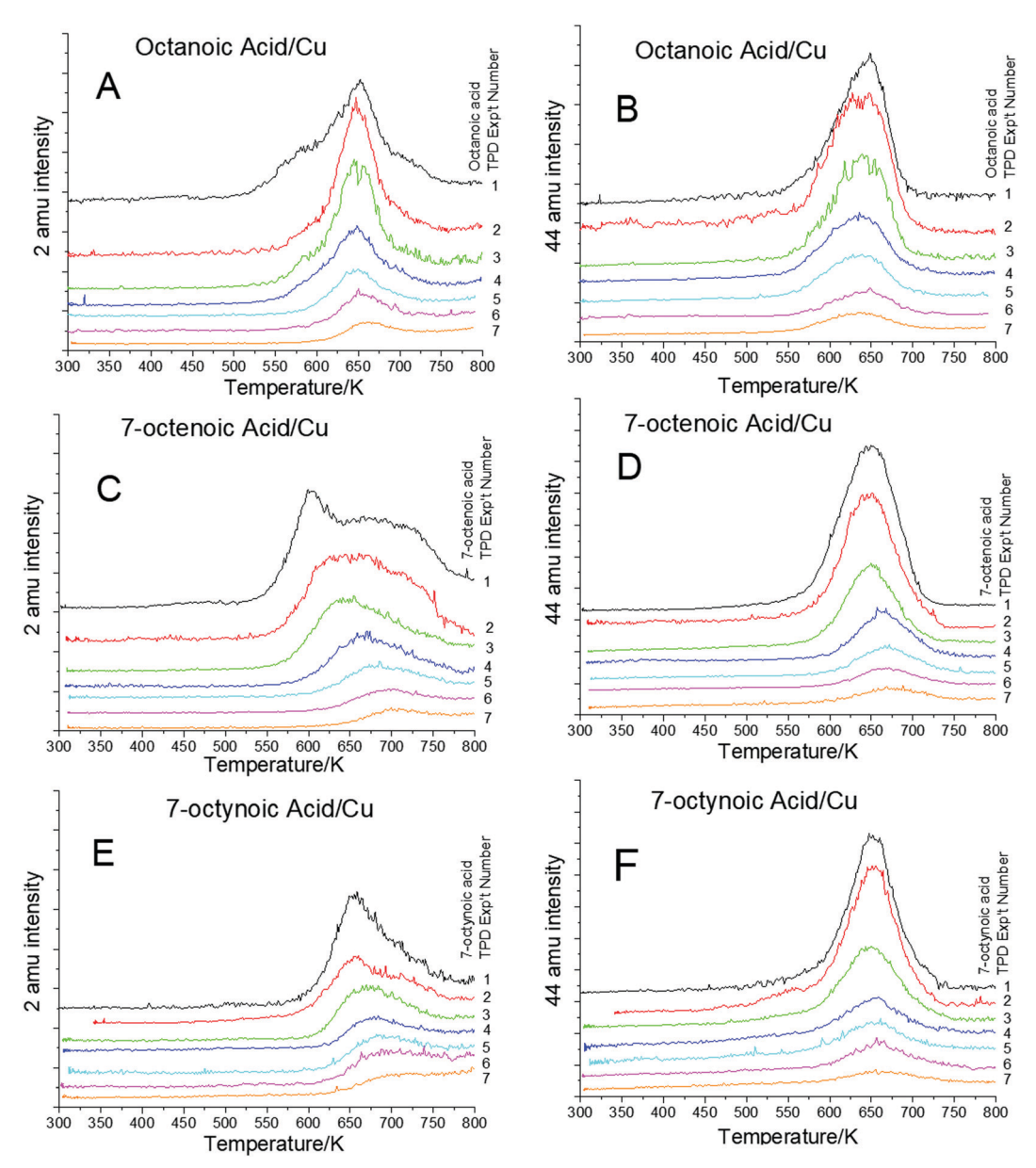


Fig. 5 Temperature-programmed desorption profiles collected while monitoring 2 amu (H₂) using a heating rate of 5 K s⁻¹ following the adsorption of a saturated overlayer of (A) octanoic acid, (C) 7-octenoic acid, (E) 7-octynoic acid. 44 amu profiles for (B) octanoic acid, (D) 7-octenoic acid, (F) 7-octynoic acid on a copper foil at 300 K and heating to 850 K and the dosed once again with the carboxylic acid. The number of adsorption and desorption cycles are displayed adjacent to the corresponding spectrum.

on the coverage, and thus on the number of vacant surface sites.

These effects are emphasized by the STM results (Fig. 4), where the amount of carbon on the surface increases with the presence of unsaturation at the chain terminus. The formation of polymeric species evident in these images is consistent with them being initiated by coupling reactions between chains. It is further confirmed by the results of the blocking experiments shown in Fig. 6, where the surface is more rapidly blocked in the order 7-octynoic > 7-octenoic > octanoic acids.

A curious difference is seen between the hydrogen evolution kinetics of heptanoic (Fig. 2A), octanoic (Fig. 2B), 6-heptynoic (Fig. 2E) and 7-octynoic (Fig. 2F) acids and the carboxylic acids terminated by vinyl groups (Fig. 2C and D) where, in the first four cases, most of the hydrogen desorbs synchronistically with carbon dioxide (Fig. 1A, B, E and F), with some additional hydrogen evolving at higher temperatures, while for 6-hepenoic and 7-octenoic acids the initial hydrogen desorption precedes decarboxylation. The origin for this effect is not clear but it does suggest that the stereochemistry of the terminal vinyl groups allows them to dehydrogenate to form relatively strong C-Cu bonds without unduly modifying the carboxylate structure, otherwise it would decompose to form carbon dioxide at lower temperatures.

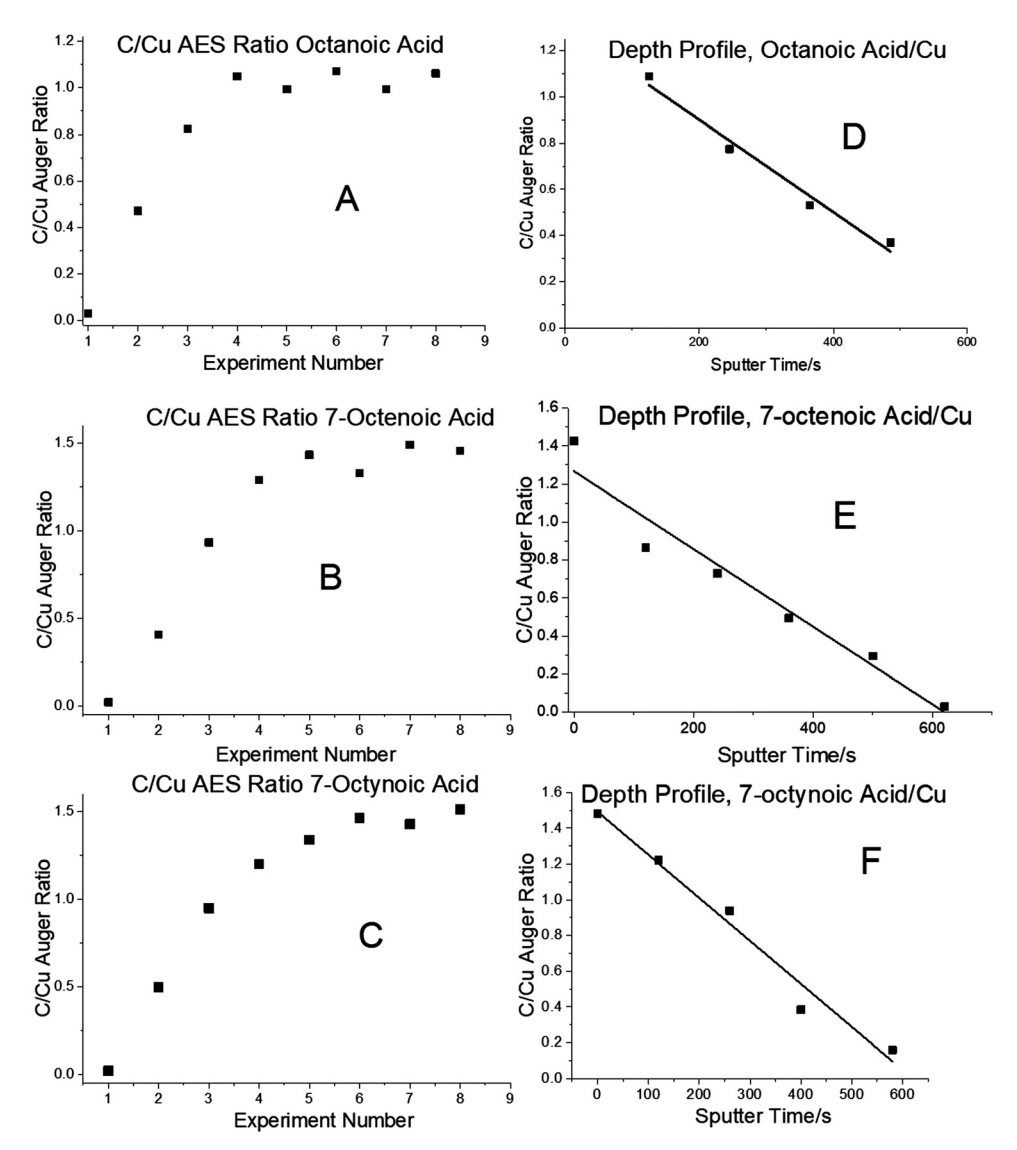


Fig. 6 Auger C/Cu peak-to-peak ratios plotted as a function of the number of adsorption-desorption cycles taken from the data in Fig. 5 for (A) octanoic acid, (B) 7-octenoic acid and (C) 7-octynoic acid on a copper foil. Plotted also are the AES C/Cu peak-to-peak ratios after seven adsorptiondesorption cycles as a function of Ar⁺ ion bombardment time using and ion beam energy of 2 keV with a sample current of 2 µA for (D) octanoic acid, (E) 7-octenoic acid and (F) 7-octynoic acid on a copper foil.

5. Conclusion

The surface chemistry of C₇ and C₈ carboxylic acids terminated by alkyl, vinyl, or alkynyl terminal groups were experimentally investigated on the copper surfaces. All carboxylic acids thermally decompose to evolve CO_2 at temperatures between ~ 500 and 700 K, depending on the coverage, with some reaction occurring at lower coverages due to an interaction of the chain terminus with the surface. However, the decarbonylation rate of the saturated overlayers does not depend on the nature of the hydrocarbon terminus, but does depend slightly on chain length. The rate of reaction of the subsequently formed carbonaceous fragment does depend on the nature of the terminal group, with the presence of unsaturation increasing the amount of carbon on the surface. This is rationalized on the basis of a competition between β-hydride elimination of the alkyl group to produce an alkene, and coupling reactions to form polymeric species on the surface. The activation barrier for the first process is less than for the second so that the relative rate of carbon deposition will increase as the temperature at which the hydrocarbon species is reactively deposited increases. Thus, the high reaction temperature of the thermally stable carboxylate group will cause relatively large amount of carbon to be deposited on the surface. This predicts that the mechanochemical decomposition of carboxylic acids on copper, which takes place at ~ 300 K, should result in the deposition of less carbon on the surface than formed in the thermal reaction, similar to the effect found for acetate species.³⁹

Conflicts of interest

There are no conflicts to declare.

Acknowledgements

We gratefully acknowledge the Civil, Mechanical and Manufacturing Innovation (CMMI) Division of the National Science Foundation under grant number CMMI-2020525 for support of this work. KH acknowledges support from the China Scholarship Council.

References

- 1 H. Sellers, A. Ulman, Y. Shnidman and J. E. Eilers, J. Am. Chem. Soc., 1993, 115, 9389-9401.
- 2 J. I. Henderson, S. Feng, G. M. Ferrence, T. Bein and C. P. Kubiak, Inorg. Chim. Acta, 1996, 242, 115-124.
- 3 T. Ishida, S. i. Yamamoto, W. Mizutani, M. Motomatsu, H. Tokumoto, H. Hokari, H. Azehara and M. Fujihira, Langmuir, 1997, 13, 3261-3265.
- 4 S. A. Swanson, R. McClain, K. S. Lovejoy, N. B. Alamdari, J. S. Hamilton and J. C. Scott, Langmuir, 2005, 21, 5034-5039.
- 5 C. Vericat, M. E. Vela and R. C. Salvarezza, Phys. Chem. Chem. Phys., 2005, 7, 3258-3268.
- 6 N. A. Kautz and S. A. Kandel, J. Am. Chem. Soc., 2008, 130, 6908-6909.
- 7 D. P. Woodruff, Phys. Chem. Chem. Phys., 2008, 10, 7211-7221.
- 8 D. K. Schwartz, Annu. Rev. Phys. Chem., 2001, 52, 107-137.
- 9 P. E. Laibinis, G. M. Whitesides, D. L. Allara, Y. T. Tao, A. N. Parikh and R. G. Nuzzo, J. Am. Chem. Soc., 1991, 113, 7152-7167.
- 10 A. Ulman, Chem. Rev., 1996, 96, 1533-1554.
- 11 B. M. Rosen and V. Percec, Nature, 2007, 446, 381-382.
- 12 K. G. Thomas and P. V. Kamat, Acc. Chem. Res., 2003, 36, 888-898.
- 13 O. Furlong, F. Gao, P. Kotvis and W. T. Tysoe, Tribol. Int., 2007, 40, 699-708.
- 14 C. A. Mirkin and M. A. Ratner, Annu. Rev. Phys. Chem., 1992, 43, 719-754.
- 15 R. Schennach, C. Hirschmugl, E. Gilli and W. T. Tysoe, Appl. Spectrosc., 2009, 63, 369-372.
- 16 S. N. Yaliraki, M. Kemp and M. A. Ratner, J. Am. Chem. Soc., 1999, 121, 3428-3434.
- 17 J. H. Schon, H. Meng and Z. Bao, Nature, 2001, 413, 713-716.
- 18 K. Komvopoulos, Wear, 1996, 200, 305-327.
- 19 R. Maboudian, W. R. Ashurst and C. Carraro, Sens. Actuators, A, 2000, 82, 219-223.
- 20 D. Clayton, Br. J. Appl. Phys., 1951, 2, 25.
- 21 F. J. Westlake and A. Cameron, Proceedings of the Institution of Mechanical Engineers, Conference Proceedings, 1967, vol. 182, pp. 75-78.

- 22 A. Tonck, J. M. Martin, P. Kapsa and J. M. Georges, Tribol. Int., 1979, 12, 209-213.
- 23 S. M. Hsu and R. S. Gates, Tribol. Int., 2005, 38, 305-312.
- 24 H. Spikes, Tribol. Lett., 2015, 60, 5.
- 25 R. Simič and M. Kalin, Appl. Surf. Sci., 2013, 283, 460-470.
- 26 M. I. De Barros Bouchet, J. M. Martin, J. Avila, M. Kano, K. Yoshida, T. Tsuruda, S. Bai, Y. Higuchi, N. Ozawa, M. Kubo and M. C. Asensio, Sci. Rep., 2017, 7, 46394.
- 27 M. Kano, J. M. Martin, K. Yoshida and M. I. De Barros Bouchet, Friction, 2014, 2, 156-163.
- 28 S. M. Lundgren, M. Ruths, K. Danerlöv and K. Persson, J. Colloid Interface Sci., 2008, 326, 530-536.
- 29 S. Campen, J. H. Green, G. D. Lamb and H. A. Spikes, Tribol. Lett., 2015, 57, 18.
- 30 M. I. De Barros Bouchet, J. M. Martin, C. Forest, T. le Mogne, M. Mazarin, J. Avila, M. C. Asensio and G. L. Fisher, RSC Adv., 2017, 7, 33120-33131.
- 31 M. Bowker and R. J. Madix, Appl. Surf. Sci., 1981, 8, 299-317.
- 32 M. Bowker and R. J. Madix, Surf. Sci., 1982, 116, 549-572.
- 33 B. A. Sexton, Chem. Phys. Lett., 1979, 65, 469-471.
- 34 D. Fuhrmann, D. Wacker, K. Weiss, K. Hermann, M. Witko and C. Woll, J. Chem. Phys., 1998, 108, 2651-2658.
- 35 M. Wühn, J. Weckesser and C. Wöll, Langmuir, 2001, 17, 7605-7612.
- 36 B. Immaraporn, P. Ye and A. J. Gellman, J. Phys. Chem. B, 2004, 108, 3504-3511.
- 37 B. Karagoz, A. Reinicker and A. J. Gellman, Langmuir, 2019, 35, 2925-2933.
- 38 R. Bavisotto, R. Rana, N. Hopper, D. Olson and W. T. Tysoe, Phys. Chem. Chem. Phys., 2021, 23, 5834-5844.
- 39 R. Rana, R. Bavisotto, N. Hopper and W. T. Tysoe, Tribol. Lett., 2021, 69, 32.
- 40 T. Kuwahara, P. A. Romero, S. Makowski, V. Weihnacht, G. Moras and M. Moseler, Nat. Commun., 2019, 10, 151.
- 41 R. Bavisotto, R. Rana, N. Hopper and W. T. Tysoe, Surf. Sci., 2021, 711, 121875.
- 42 T. Kravchuk, L. Vattuone, L. Burkholder, W. T. Tysoe and M. Rocca, J. Am. Chem. Soc., 2008, 130, 12552-12553.
- 43 N. R. Avery, J. Am. Chem. Soc., 1985, 107, 6711-6712.
- 44 T. B. Creczynski-Pasa, M. A. D. Millone, M. L. Munford, V. R. de Lima, T. O. Vieira, G. A. Benitez, A. A. Pasa, R. C. Salvarezza and M. E. Vela, Phys. Chem. Chem. Phys., 2009, 11, 1077-1084.
- 45 E. Torres, A. T. Blumenau and P. U. Biedermann, Chem-PhysChem, 2011, 12, 999-1009.
- 46 B. E. Bent, Chem. Rev., 1996, 96, 1361-1390.
- 47 C. J. Jenks, C. M. Chiang and B. E. Bent, J. Am. Chem. Soc., 1991, 113, 6308-6309.
- 48 C. J. Jenks, B. E. Bent and F. Zaera, J. Phys. Chem. B, 2000, **104**, 3017-3027.